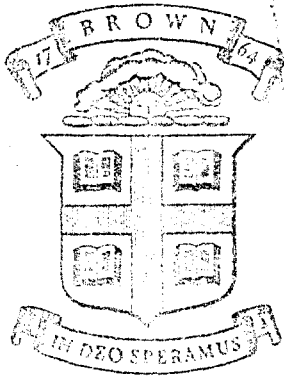


AD-734176

Division of Engineering
BROWN UNIVERSITY
PROVIDENCE, R. I.



Reproduced From
Best Available Copy

ELASTIC ANALYSIS OF A SKULL

C. H. HARDY and P. V. MARÇAL

D D C
RECEIVED
DEC 28 1971
REGISTERED
C

Office of Naval Research
Department of the Navy
Contract No. N00014-67-A-0191-0007
Task Order NR 064-512
Technical Report No. 8

Reproduced by
NATIONAL TECHNICAL
INFORMATION SERVICE
Springfield, Va. 22151

N00014-0007/8

November 1971

UNCLASSIFIED
EXCEPT WHERE SHOWN
OTHERWISE

28

ELASTIC ANALYSIS OF A SKULL

by

Claude H. Hardy and Pedro V. Marcal
Division of Engineering, Brown University
Providence, Rhode Island 02912

ABSTRACT

A finite element elastic analysis is made of a skull. Measurements were made of the geometry and thickness of a skull. The skull was then idealized with a doubly curved and arbitrary triangular shell element. Results suggest that the skull is well built for resistance to front loads. The importance of using a composite material through the thickness of the shell was established. On the basis of tensile cracking at maximum elastic stress, loads of 3,500 lbs. and 1,400 lbs. were predicted for the first cracking of the skull due to front and side loading respectively.

Reproduction in whole or in part is permitted for
any purpose of the United States Government.

Unclassified

Security Classification

DOCUMENT CONTROL DATA - R & D

(Security classification of title, body of abstract and indexing annotation must be entered when the overall report is classified)

1. ORIGINATING ACTIVITY (Corporate author) Brown University Division of Engineering		2a. REPORT SECURITY CLASSIFICATION Unclassified	
		2b. GROUP N/A	
3. REPORT TITLE Elastic Analysis of a Skull			
4. DESCRIPTIVE NOTES (Type of report and inclusive dates) Technical Report			
5. AUTHOR(S) (First name, middle initial, last name) Claude H. Hardy and Pedro V. Marcal			
6. REPORT DATE November 1971		7a. TOTAL NO. OF PAGES 25	7b. NO. OF REFS 10
8a. CONTRACT OR GRANT NO. N00014-67-A-0191-0007		8a. ORIGINATOR'S REPORT NUMBER(S) N00014-0007/8	
b. PROJECT NO. NR 064-512			
c.		8b. OTHER REPORT NO(S) (Any other numbers that may be assigned this report)	
d.			
10. DISTRIBUTION STATEMENT Reproduction in whole or in part is permitted for any purpose of the United States Government.			
11. SUPPLEMENTARY NOTES		12. SPONSORING MILITARY ACTIVITY Office of Naval Research Boston Branch Office, 495 Summer Street Boston, Massachusetts 02210	
13. ABSTRACT A finite element elastic analysis is made of a skull. Measurements were made of the geometry and thickness of a skull. The skull was then idealized with a doubly curved and arbitrary triangular shell element. Results suggest that the skull is well built for resistance to front loads. The importance of using a composite material through the thickness of the shell was established. On the basis of tensile cracking at maximum elastic stress, loads of 3,500 lbs. and 1,400 lbs. were predicted for the first cracking of the skull due to front and side loading respectively.			

14. KEY WORDS	LINK A		LINK B		LINK C	
	ROLE	WT	ROLE	WT	ROLE	WT
Structural Analysis						
Crashworthiness Study						
Biomechanics						
Skull Injury						
Elastic Analysis						

Introduction

In recent years much attention and concern has been focused on the hazards introduced by our two most significant means of transportation, viz. the automobile and the airplane. In automobile and airplane accidents, serious injuries involving the head occur most frequently. Kihlberg [1,2] for instance has estimated that the head is involved in about 70% of all motor accidents. Yet little is known about the exact causes of injuries to the head and the interaction of the skull, brain and central nervous system. Goldsmith [3] has discussed the causes of injury of the head from the point of view of biomechanics. The causes leading to such head injuries were divided into three categories:

- 1) A direct impact or blow,
- 2) An indirect impulsive load due to sudden deceleration, and
- 3) Quasi-static loading produced by relatively long-time crushing.

Perrone [4] in a recent report considered design against impact damage by energy absorbing devices. The basic idea of these devices is to absorb the energy in a controlled manner. Since the energy being absorbed is in most cases stored in the head, it is important to know the level of loading that the head can tolerate. It is recognized that the brain is the ultimate portion that decides whether injury has been caused to the head. However, a knowledge of the ultimate loads on a skull places an upper bound on the behavior of the whole head system. In this report we shall consider only the loading of the skull. Another reason for considering the skull is that the severity of damage to the skull is sometimes judged on the basis of the existence of a line crack. A knowledge of the stress picture may therefore help in placing a load level on the first cracking of a skull. In this report, we shall examine the behavior of the skull subjected to quasi-static loading. We shall assume elastic isotropic behavior in the plane of the skull. It will be shown later that the variation of the elastic modulus through the thickness has an important bearing on the level of stresses that are predicted.

Theoretical Considerations

In this work we have made use of the finite element method. A doubly curved triangular shell element due to Dupuis [5] was used in a general purpose program [6]. The basic features of the shell element are shown in Fig. 1. The element is a three node triangular isoparametric element with nine degrees of freedom at each node. Two sets of coordinates are used to describe the geometry of an element viz. the Cartesian x, y, z and the Gaussian θ_1, θ_2 coordinates. Thus geometry of the shell element is specified by giving $\theta_1, \theta_2, x, \frac{\partial x}{\partial \theta_1}, \frac{\partial x}{\partial \theta_2}, y, \frac{\partial y}{\partial \theta_1}, \frac{\partial y}{\partial \theta_2}, z, \frac{\partial z}{\partial \theta_1}, \frac{\partial z}{\partial \theta_2}$, at the nodes. Because this is an isoparametric element the degrees of freedom at each node is correspondingly, $u, \frac{\partial u}{\partial \theta_1}, \frac{\partial u}{\partial \theta_2}, v, \frac{\partial v}{\partial \theta_1}, \frac{\partial v}{\partial \theta_2}, w, \frac{\partial w}{\partial \theta_1}, \frac{\partial w}{\partial \theta_2}$. The element is based on a cubic interpolation function with rational functions added to enforce compatibility at the boundaries. The same interpolation function is used for all directions, u, v, w . Only a constant thickness can be specified for each element. However, because of the composite nature of the skull bone the program was modified to allow a variation of the modulus through the thickness in order to simulate the diploe and the outer and inner table.

Model of Skull and Loading

In this analysis we have only considered the skull. The contents of the skull has been ignored. Since it was possible to obtain a large variation between skull dimensions [7], it was decided to concentrate the analysis on a single skull and leave a parametric study to a subsequent project. A triangular mesh was first inscribed on a skull and measurements of its Cartesian coordinates were made by means of a traveling microscope. A micrometer survey was also performed to find the average thickness of each region of the skull. The mesh pattern is shown in Figs. 2 and 3. Table 1 summarizes the thickness survey. A program was then written to obtain the necessary coordinate and rates of change of coordinates data for use in defining the element.

Two analyses were performed on the model with one a front pressure load and the other a side load. The pressure loads were applied on elements 28 and 29 and elements 36 and 37 respectively.

Boundary conditions were applied so as to enforce symmetry about half the skull. In addition nodal point 29 was fixed in all three directions u , v and w and nodal point 21 was fixed in the u direction to prevent rotation. The u , v and w displacement directions correspond to the x , y and z axis respectively and these axis directions are shown in Figs. 4 and 5. The boundary conditions on nodes 29 and 21 are somewhat artificial since resistance to loads is effected either by inertia effects and hence more diffuse or by transmission to the body via the neck. It was however thought that the manner of support would not affect the stresses near the loaded region.

The two analyses were first performed on models with uniform material through the thickness. An examination of the results suggested that the skull was surprisingly strong. This led to speculation on the effect of the presence of the diploe. The skull was again analyzed as a three-layer composite shell. A quarter of the thickness on the outside and also on the inside was assumed to represent the outer and inner table with a modulus of four times ($E = 6.0 \times 10^5$ lbs/in²) that of the central diploe ($E = 1.5 \times 10^5$ lbs/in²).

Numerical Results

Uniform Material Through the Thickness

Front Load: The following results were obtained for a pressure load corresponding to a 1000 lb. load on the front of the skull. An equivalent modulus of 200,000 lbs/in² was assumed [8]. Half of the load was applied on elements 28 and 29 which had a combined surface area of 1.1 in².

Figure 4 shows the variation of displacement around a horizontal section of the skull cap while Fig. 5 gives the variation of displacement around the

Saggital or mid-section. Figures 6 and 7 give the equivalent stress on the outer and inner surface of the horizontal and Saggital section of the skull.

Side Load: The results are shown for a load of 1000 lbs. applied to elements 36 and 37 on the side of the skull. The full load was applied to an area of about 1.44 in².

Figures 8 and 9 give the variations of displacement for this load and Figs. 10 and 11 show the equivalent stresses induced by the loading.

Composite Material Through the Thickness

Front Load: The analysis was repeated for the case of the front load. This time the inner and outer table were simulated with a modulus four times that of the diploe. The thickness of the diploe was allowed to take on the values of 0.5 and 0.66 of the skull thickness.

Side Load: The analysis was also repeated for the side load case. Here a 0.5 diploe/thickness ratio was used. Figure 14 gives the stress distribution on the horizontal section.

Finally Table 2 gives the maximum stresses encountered in the region near the applied loads. The stresses were mainly compressive with a bending stress superimposed on a high compressive membrane stress.

Discussion

The most striking feature of the results is the very rapid transition of the bending stress states in the shell to a membrane state. The skull appears to be well 'designed' for front loads. A comparison of Figs. 7 and 10 shows that the skull is more severely stressed when loaded in the side.

An examination of Table 2 shows the importance of considering the skull as made up of a composite shell. In thickness surveys of the cranial bone, the inner

and outer table were not found to vary in proportion to the variation in thickness. The inner and outer table remained almost constant with increase of thickness.

The relative moduli and thicknesses of the layers obviously have a great effect on the skull stresses. In order to study the sensitivity of the stresses to these parameters it was first decided to fix the diploe to skull thickness ratio at 0.5. Because the inner and outer table do not increase significantly with overall thickness, this ratio increases to about 0.66 in thicker sections. The frontal load analysis subjects the thicker sections of the skull to high stresses so that the final analysis was made with a composite shell with one sixth the thickness on either side representing the inner and outer table.

In future analysis where deflections may be important it will be necessary to include a variable diploe to thickness ratio for each element in the skull. This will require further modification of the program. With the constant diploe to thickness ratios used in the analysis the maximum tensile stresses increased by 40% and 30% in the front and side load case, respectively. This establishes the importance of treating the skull as a composite shell.

The failure loads predicted on the basis of a maximum tensile stress of 7500 lbs/in² [9] are shown in Table 3. On this basis the skull in a front load situation is able to resist 2.5 times the load that it can resist in a side load situation. The maximum displacement corresponding to the failure load is also shown in Table 3. The difference between the maximum displacements in the isotropic and the composite shell analysis may be explained by the difference in the values of the assumed Young's Modulus. The predicted failure loads are 3500 lbs. and 1400 lbs. for the front and side load respectively. This load is surprisingly high but is consistent with the range of the energy (400-900 lb.-in.) required to fracture cadaver skulls [10]. On the basis of these elastic loading to tensile

failure results, it would appear that the structure of the skull need not be considered in considering brain damage. The damage to the internal brain matter can be expected before the 3500 and 1400 lbs. required to cause fracture of the skull. However, the predicted displacements at fracture are of the order of 0.2 ins. and 0.34 ins. and this displacement may affect the brain either by extruding it out of the foramen magnum at the base of the skull or by imparting vibrational movement to the brain. It is now useful to consider the loads found here also to be an estimate of the load required for the first appearance of a line crack. Since this has been observed to occur with the onset of concussion, it is interesting to speculate that the brain is well packaged and supported in the skull.

Finally, it is interesting to note that, in the case of the front load, the compressive yield stress is reached at the same time as the maximum tensile stress. This is another example of the optimization of a structure in nature.

Conclusions and Future Work

A linear elastic finite element analysis was performed on a model of the skull. Results suggest that the skull is well built for resistance to front loads. The side of the skull is less resistant to load. The importance of using a composite shell model for the skull analysis was established. On the basis of tensile cracking, a load of 3500 lbs. and 1400 lbs. was predicted for the first cracking of the skull due to front and side loading. This result is consistent with experimental observations of the energy required to cause fracture in cadaver skulls.

Future work should be concerned with the effect of dynamic loads on the complete skull brain structure.

Acknowledgments

The authors are grateful to Dr. Perrone of the Office of Naval Research for the initial suggestion of the problem and also for many useful discussions.

Table 1. Thicknesses at location of nodes,
Brown Biomedical Center Skull #27

<u>Node</u>	<u>h (inches)</u>	<u>Node</u>	<u>h (inches)</u>
1	0.210	24	0.215
2	0.255	25	0.125
3	0.265	26	0.210
4	0.225	27	0.170
5	0.280	28	0.165
6	0.265	29	0.300
7	0.265	30	0.100*
8	0.345	31	0.060*
9	0.190	32	0.110*
10	0.250	33	0.050*
11	0.225	34	0.285
12	0.275	35	0.235
13	0.195	36	0.515
14	0.305	37	0.870*
15	0.260	38	0.100*
16	0.280	39	0.600*
17	0.203	40	0.210
18	0.188	41	0.185
19	0.155	42	0.450
20	0.253	43	0.120*
21	0.232	44	0.120*
22	0.290*	45	0.120*
23	0.290		

* in certain regions, e.g., the skull base, it was not possible to define a thickness; therefore these figures are only rough approximations.

Load	Maximum Compressive Stress lbs/in ²	Maximum Tensile Stress lbs/in ²	Shell Material
Front pressure	-2600	1500	Isotropic
Side pressure	-6000	4050	Isotropic
Front pressure	-3600	1850	0.5 diploe/thick.
Side pressure	-8300	5200	0.5 diploe/thick.
Front pressure	-4200	2120	0.66 diploe/thick.

Table 2. Meridional Stresses due to 1000 lb. load.

Load	Shell Material	Failure Load in Tension, lbs.	Maximum Displacement at Failure, ins.	Elastic Energy at Failure, lb.-ins.
Front Pressure	Isotropic	5000	0.48	1200
	0.5 diploe/thick.	4300	0.21	450
	0.66 diploe/thick.	3500	0.20	350
Side Pressure	Isotropic	1900	0.27	256
	0.5 diploe/thick.	1400	0.34	476

Table 3. Failure Loads and Maximum Displacements

References

1. Kihlberg, J. K., "Head Injury in Automobile Accidents," Head Injury Conference Proceedings, J. B. Lippincott, Philadelphia, 1966, pp. 27-36.
2. Kihlberg, J. K., "Multiplicity of Injury in Automobile Accidents," Impact Injury and Crash Protection, C. C. Thomas, Springfield, 1970, pp. 5-24.
3. Goldsmith, W., "Biomechanics of Head Injury," Lecture Notes, University of California, Berkeley.
4. Perrone, N., "Crashworthiness and Biomechanics of Vehicle Impact," Proc. ASME Winter Annual Meeting, Dynamic Response of Biomechanical Systems, New York, 1970.
5. Dupuis, G. A., "Application of Ritz's Method to Thin Elastic Shells Analysis," Brown University, Division of Engineering, Report N00014-0008/1, July 1970.
6. Hibbitt, H. D., Levy, N. J. and Marcal, P. V., "General Purpose Programs for Nonlinear Finite Element Analysis," Proc. Seminar on General Purpose Finite Element Computer Programs, ASME Winter Annual Meeting, New York, December 1970.
7. Hubbard, R. P., "Flexure of Layered Cranial Bone," Proc. ASME Winter Annual Meeting, Paper No. 70-WA/BHF-5, New York, December 1970.
8. Perrone, N., Private Communication, August 1971.
9. Wood, J. L., "Tensile Properties of Bone at High Strain Rates," Proc. ASME Winter Annual Meeting, Paper No. 70-WA/BHF-10, New York, December 1970.
10. Hirsch, A. E., "Current Problems in Head Protection," Head Injury Conference Proceedings, J. B. Lippincott, Philadelphia, 1966, pp. 37-40.

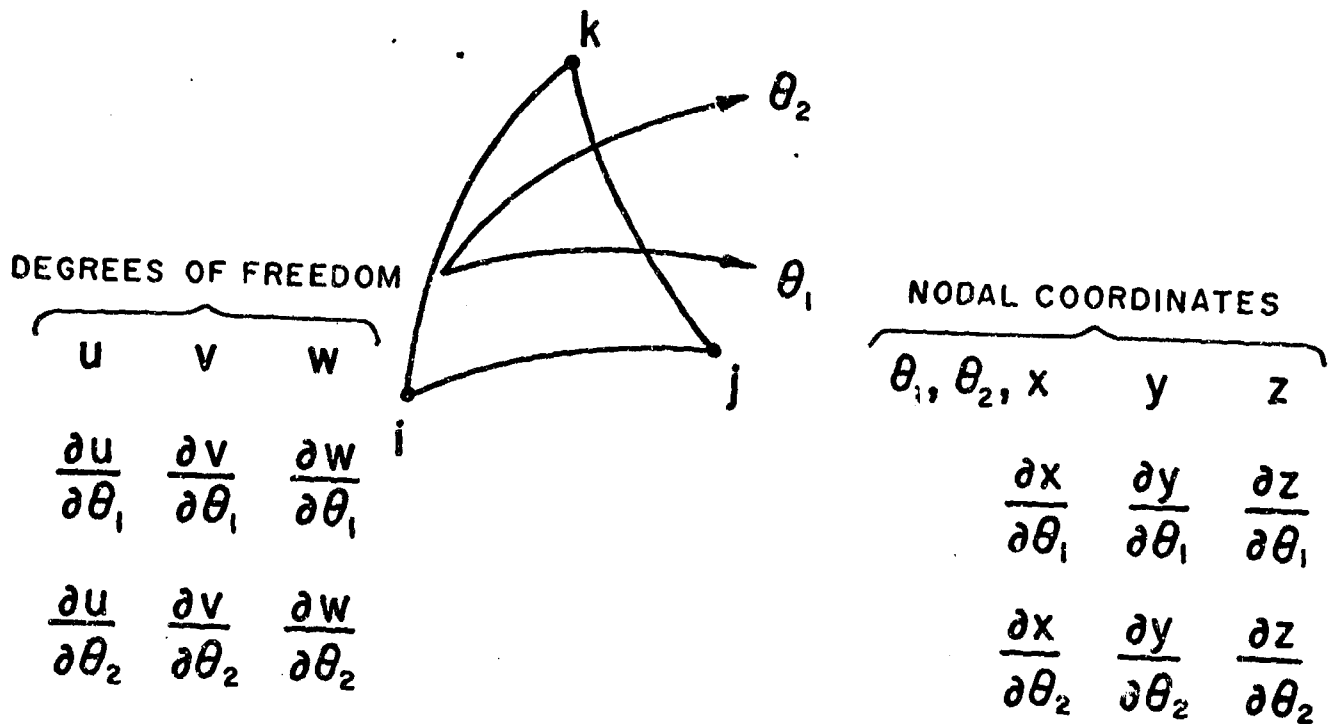


FIG. 1 TRIANGULAR SHELL ELEMENT WITH NONORTHOGONAL GAUSSIAN COORDINATES.

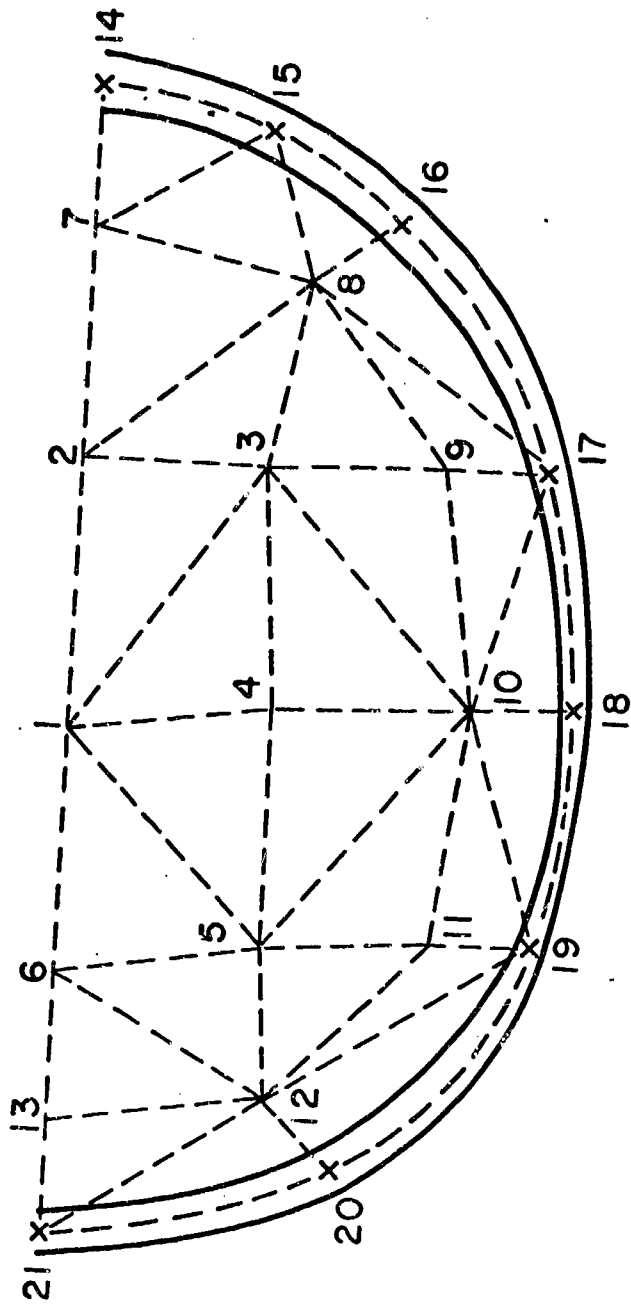
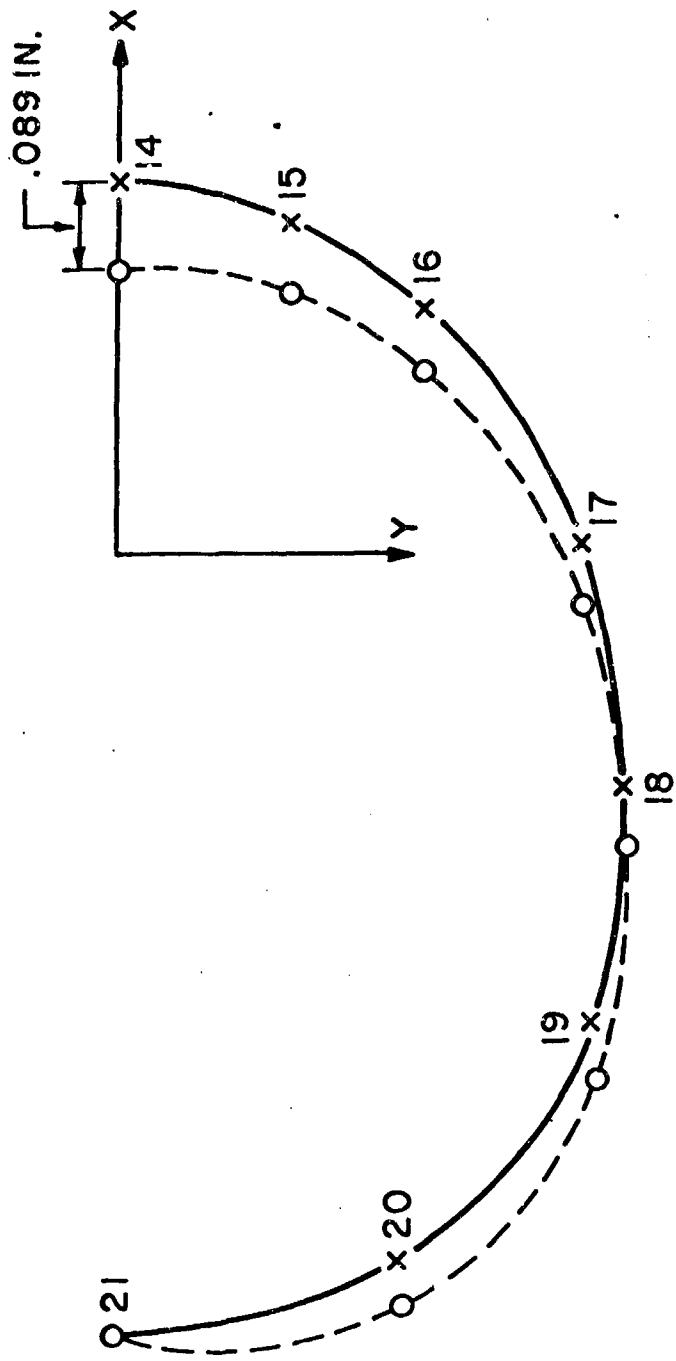


FIG. 3 HORIZONTAL SECTION THROUGH THE SKULL CAP.



SCALE: DISPLACEMENT

$\overline{\hspace{1.5cm}}$
0.184 IN.

FIG. 4 DISPLACEMENT OF HORIZONTAL SECTION, FRONT LOAD.

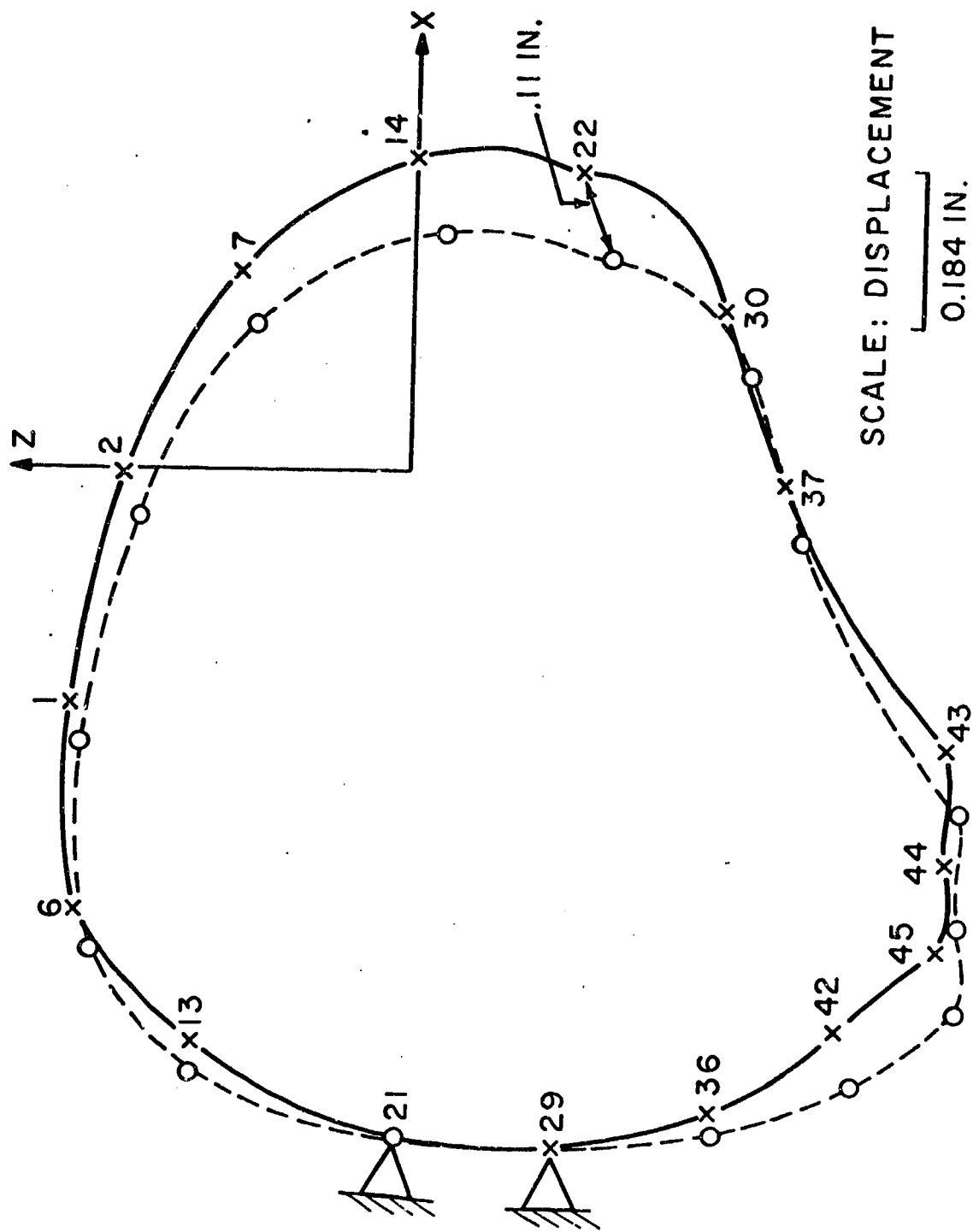


FIG. 5 DISPLACEMENT OF SAGITTAL SECTION, FRONT LOAD.

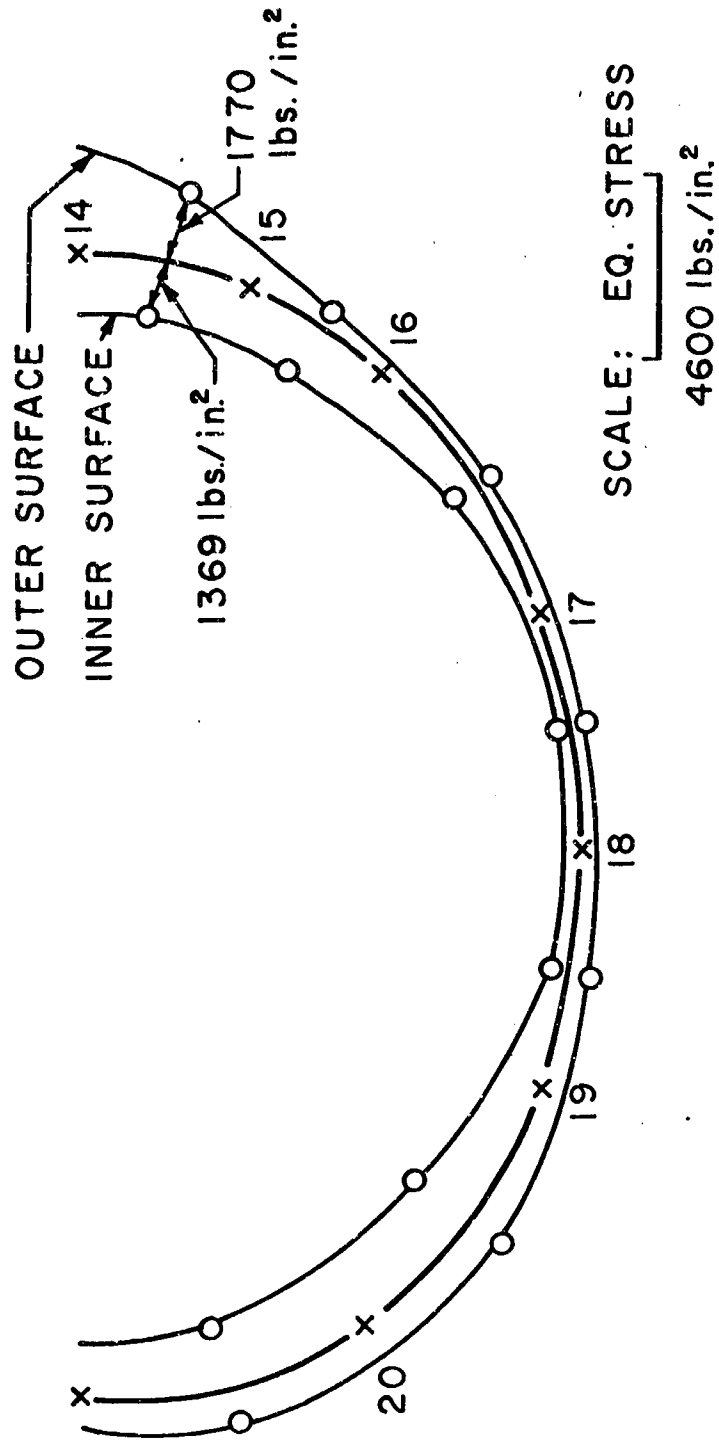


FIG. 6 EQUIVALENT STRESS ON OUTER AND INNER SURFACE,
FRONT LOAD.

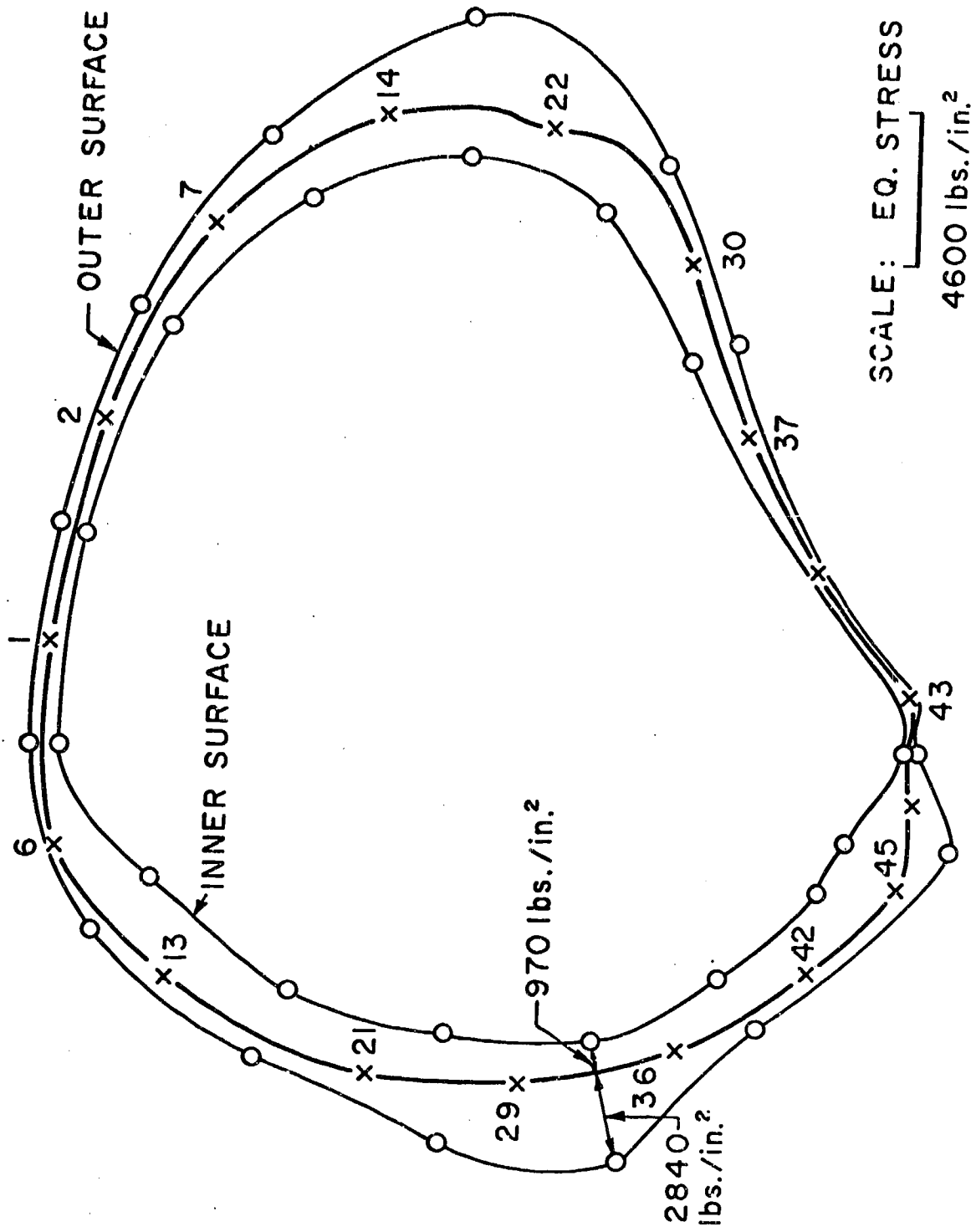


FIG. 7 EQUIVALENT STRESS ON OUTER AND INNER SURFACE, FRONT LOAD.

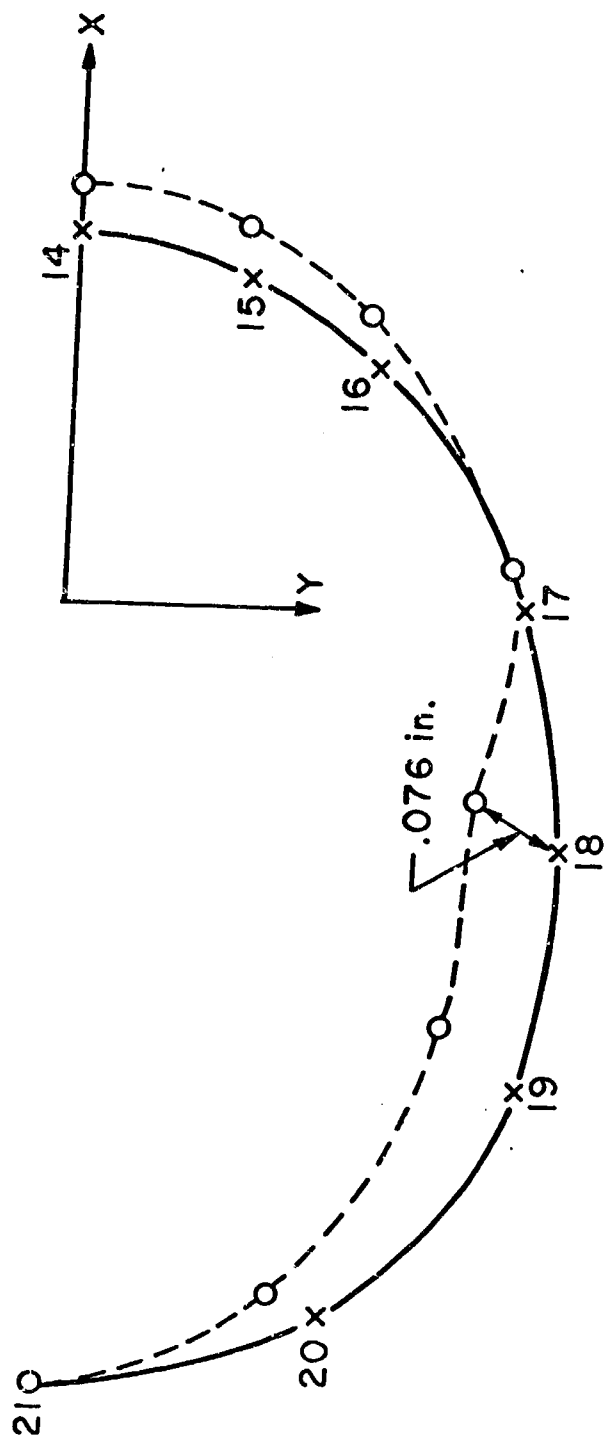


FIG. 8 DISPLACEMENT OF HORIZONTAL SECTION, SIDE LOAD.

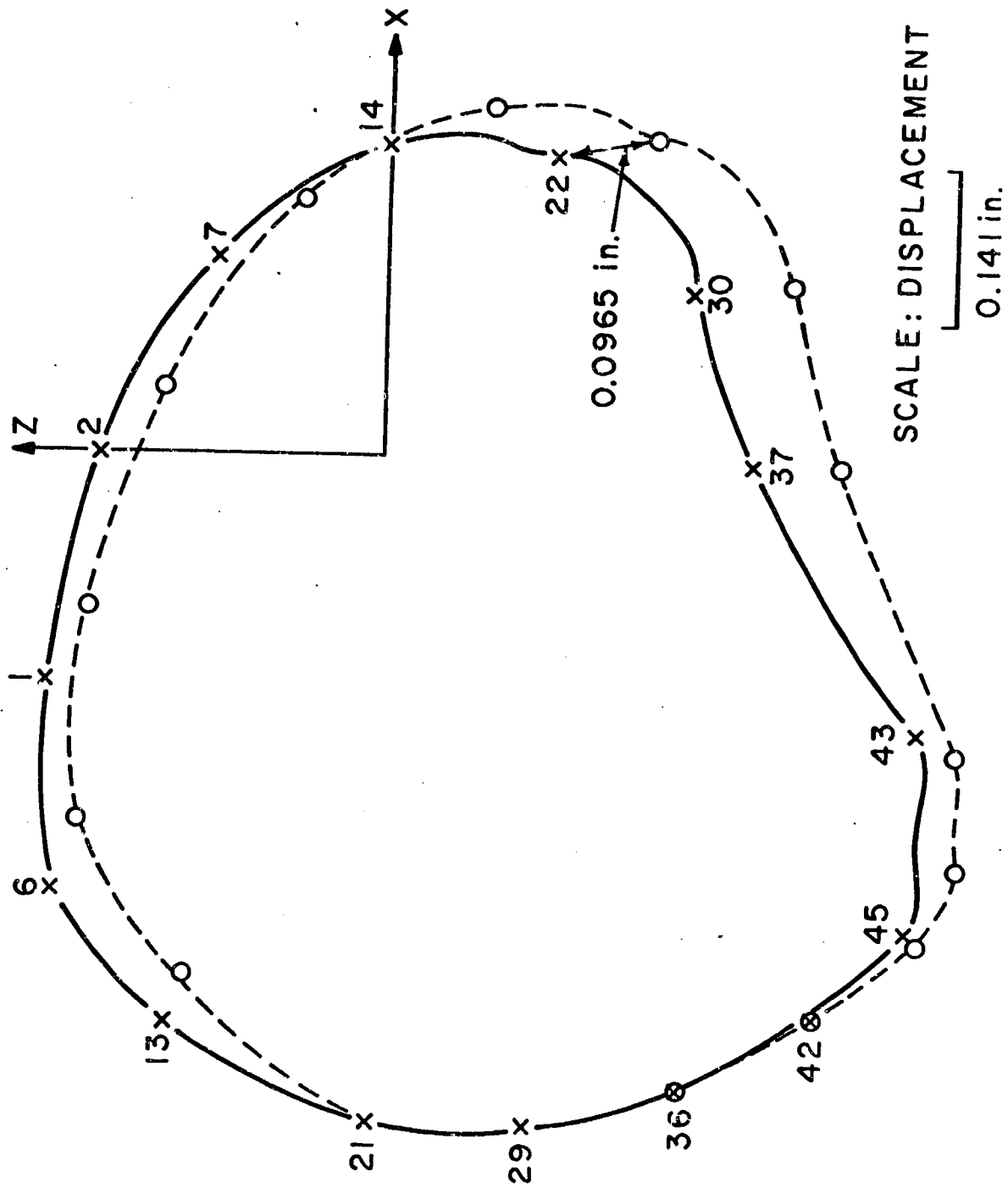


FIG. 9 DISPLACEMENT OF SAGITTAL SECTION, SIDE LOAD.

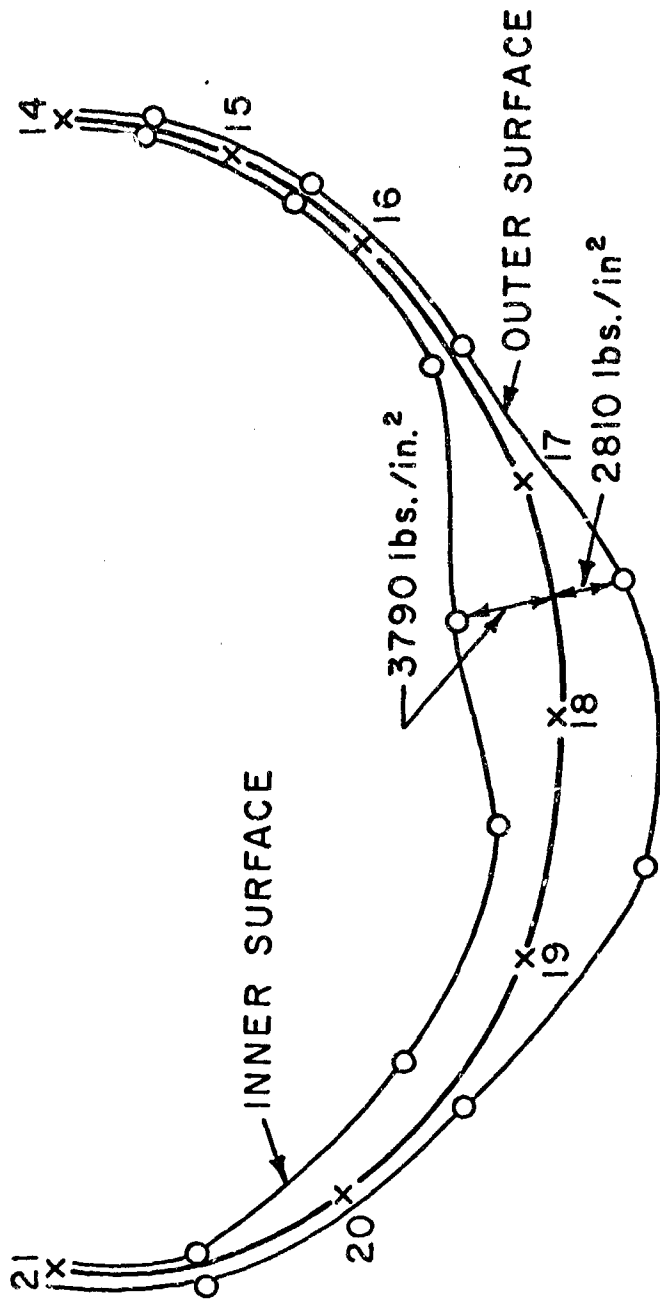


FIG. 10 EQUIVALENT STRESS ON HORIZONTAL SECTION,
SIDE LOAD.

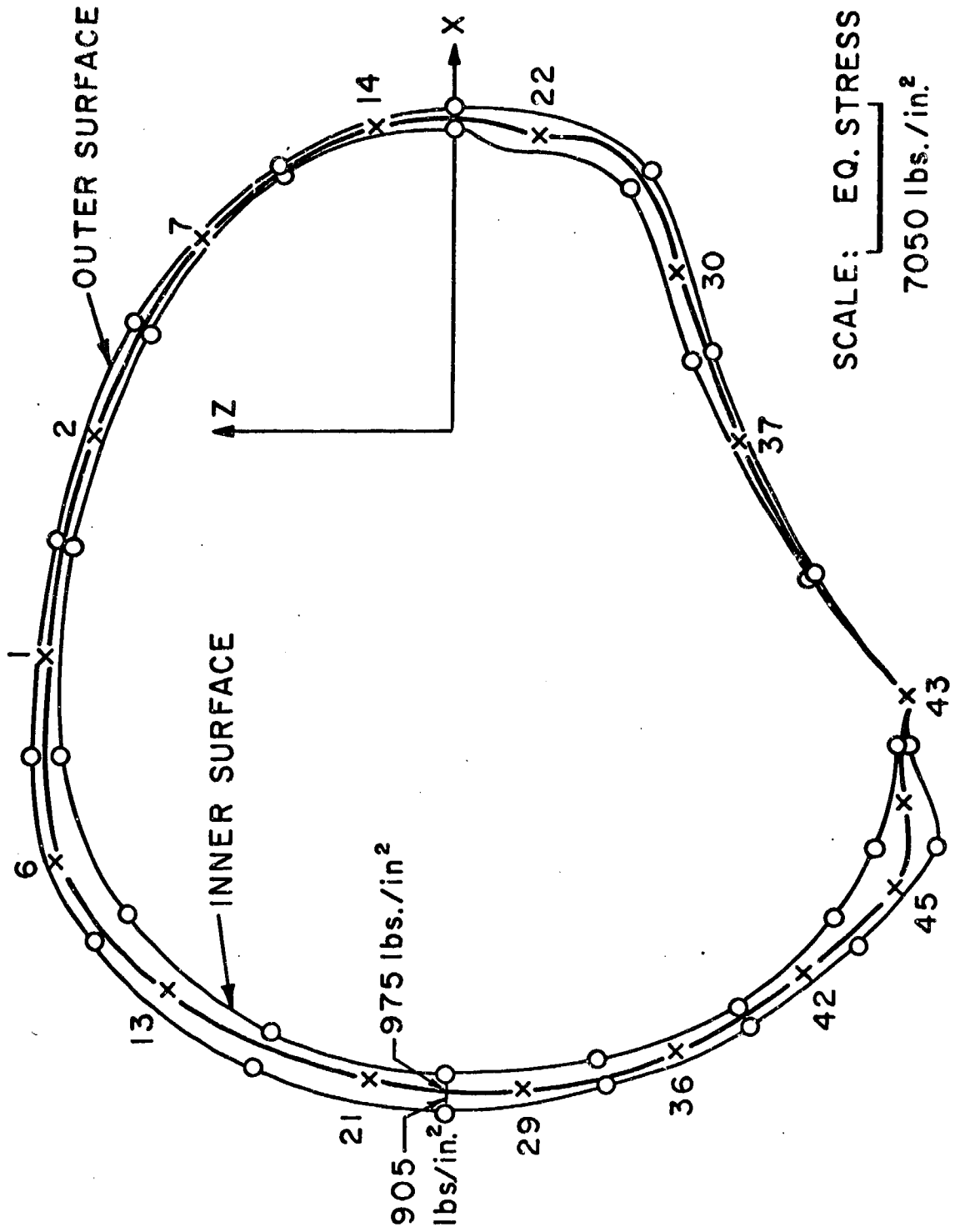


FIG. 11 EQUIVALENT STRESS ON SAGITTAL SECTION, SIDE LOAD.

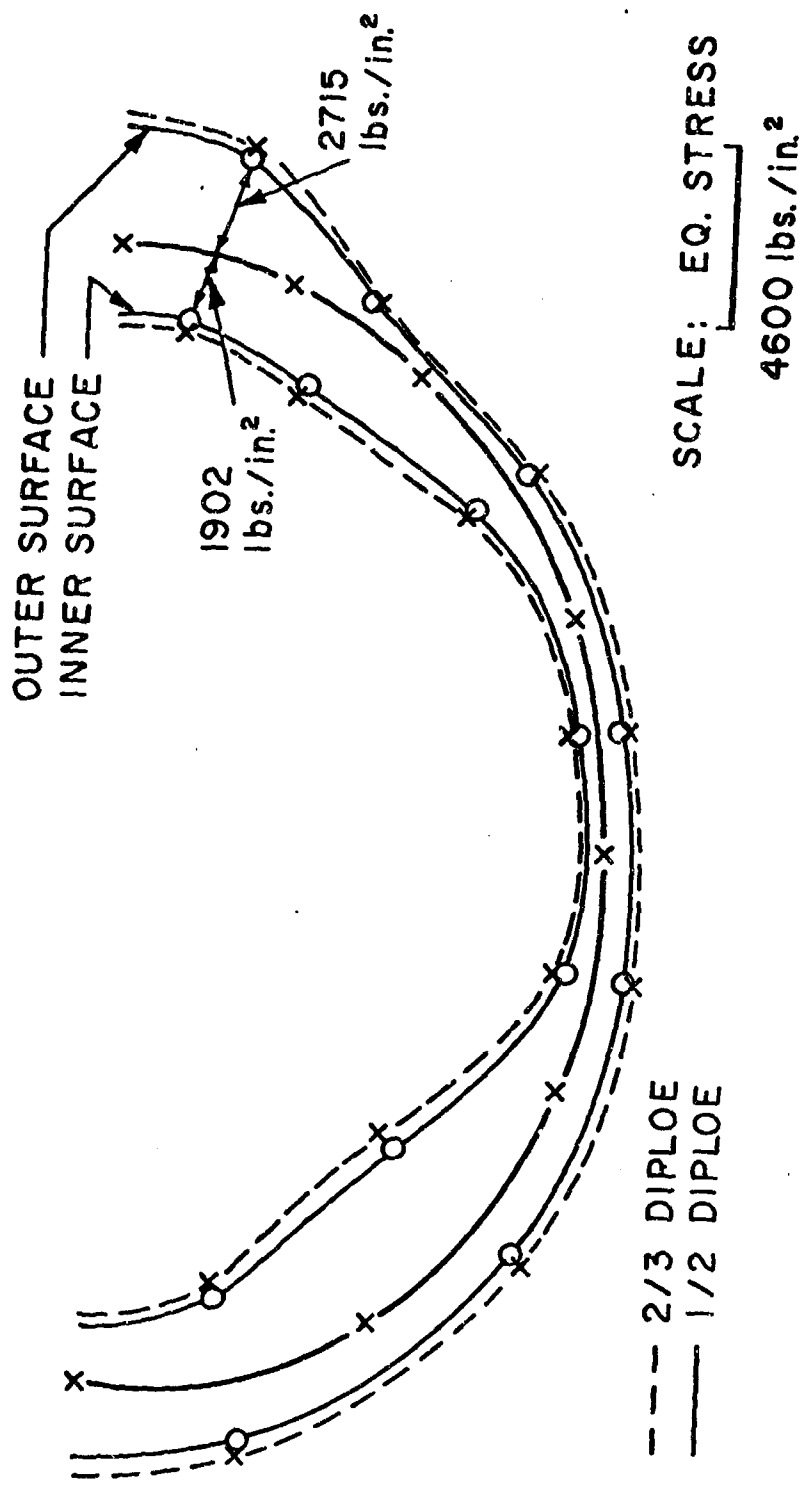


FIG. 12 EQUIVALENT STRESS ON HORIZONTAL SECTION, FRONT LOAD.

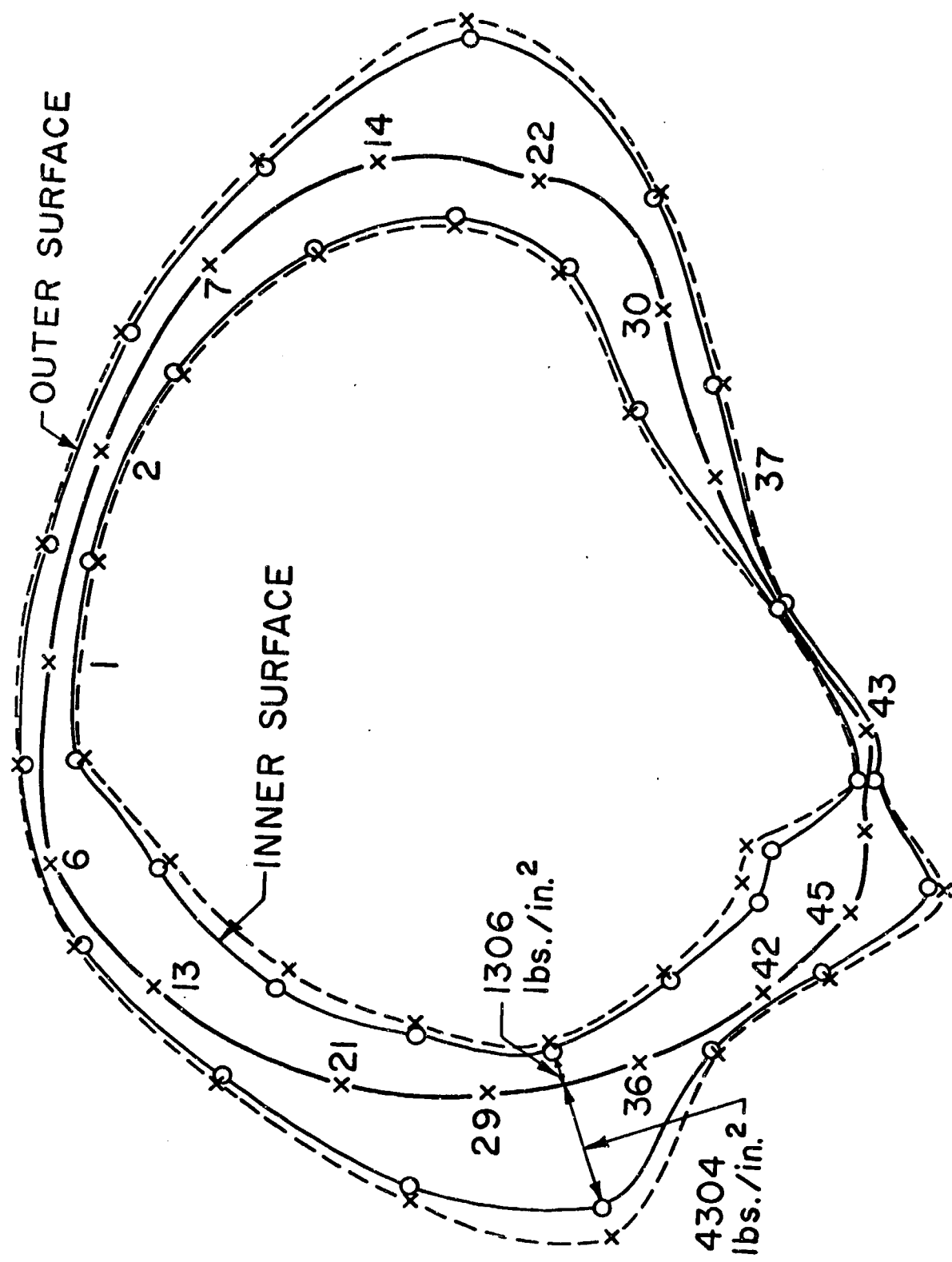


FIG. 13 EQUIVALENT STRESS ON SAGITTAL SECTION, FRONT LOAD.

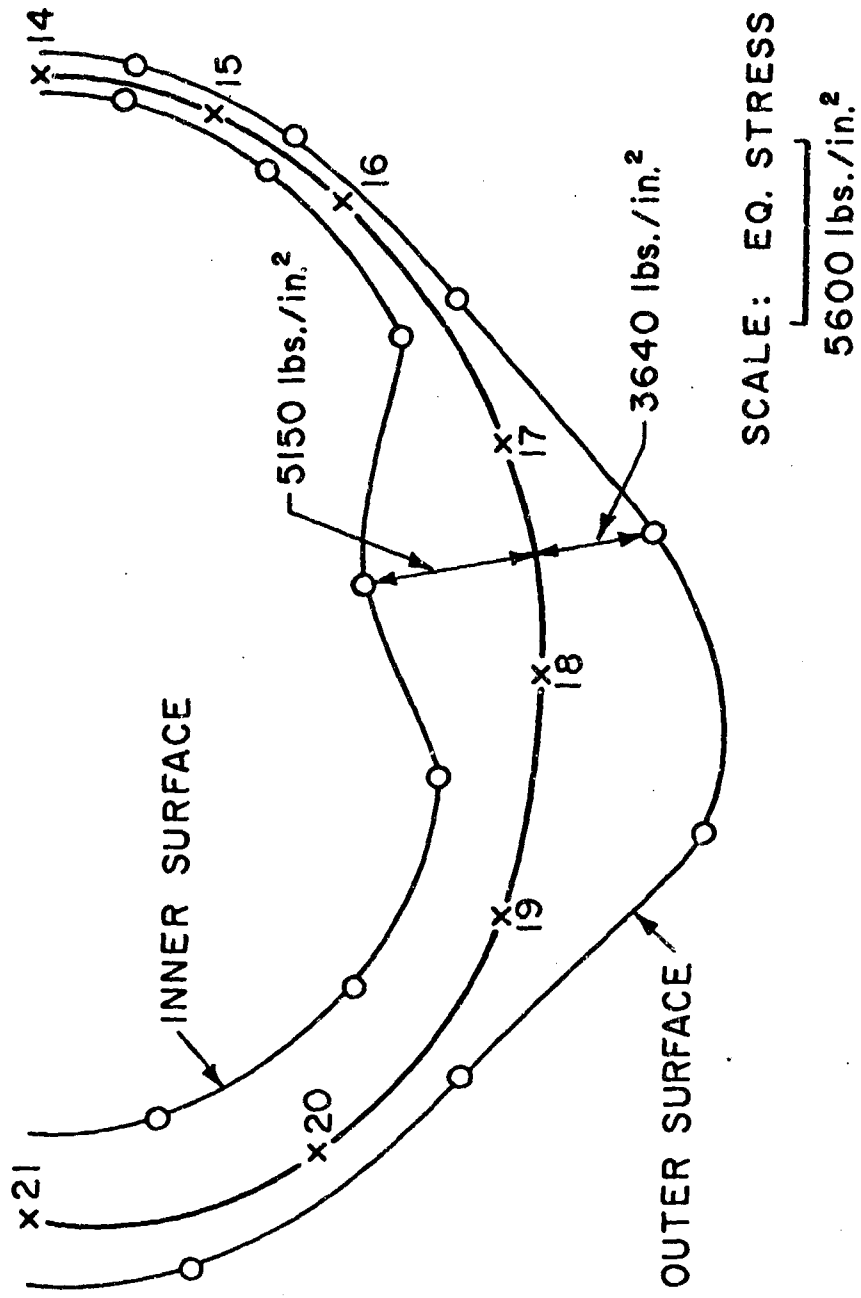


FIG. 14 EQUIVALENT STRESS ON HORIZONTAL SECTION,
SIDE LOAD.